

Article

# Surface Modification of TiO<sub>2</sub> for Obtaining High Resistance against Poisoning during Photocatalytic Decomposition of Toluene

Byeong Jun Cha <sup>1</sup>, Tae Gyun Woo <sup>1</sup>, Sang Wook Han <sup>1</sup>, Shahid Saqlain <sup>1</sup>, Hyun Ook Seo <sup>2,\*</sup>, Hong Kwan Cho <sup>3</sup>, Jee Yong Kim <sup>3</sup> and Young Dok Kim <sup>1,\*</sup>

<sup>1</sup> Department of Chemistry, Sungkyunkwan University, Suwon 16419, Korea; ckqudwms223@gmail.com (B.J.C.); tkwoo21@gmail.com (T.G.W.); swhan8905@gmail.com (S.W.H.); shahidsaqlain@hotmail.com (S.S.)

<sup>2</sup> Department of Chemistry and Energy Engineering, Sangmyung University, Seoul 03016, Korea

<sup>3</sup> Samsung Electronics Co., Ltd., Suwon 16677, Korea; hk81.cho@samsung.com (H.K.C.); jeeyong.kim@samsung.com (J.Y.K.)

\* Correspondence: hyun.ook.seo@smu.ac.kr (H.O.S.); ydkim91@skku.edu (Y.D.K.); Tel.: +82-010-3555-3164 (H.O.S.); +82-010-9163-8045 (Y.D.K.)

Received: 6 October 2018; Accepted: 24 October 2018; Published: 26 October 2018



**Abstract:** Titanium oxide (TiO<sub>2</sub>) nanostructures, the most widely used photocatalysts, are known to suffer from poisoning of the active sites during photocatalytic decomposition of volatile organic compounds. Partially oxidized organic compounds with low volatility stick to the catalyst surface, limiting the practical application for air purification. In this work, we studied the UV-driven photocatalytic activity of bare TiO<sub>2</sub> toward toluene decomposition under various conditions and found that surface deactivation is pronounced either under dry conditions or humid conditions with a very high toluene concentration (~442 ppm). In contrast, when the humidity was relatively high (~34 %RH) and toluene concentration was low (~66 ppm), such deactivation was not significant. We then modified TiO<sub>2</sub> surfaces by deposition of polydimethylsiloxane and subsequent annealing, which yielded a more hydrophilic surface. We provide experimental evidence that our hydrophilic TiO<sub>2</sub> does not show deactivation under the conditions that induce significant deactivation with bare TiO<sub>2</sub>. Conversion of toluene into dimethylacetamide was observed on the hydrophilic TiO<sub>2</sub> and did not result in poisoning of active sites. Our hydrophilic TiO<sub>2</sub> shows high potential for application in air purification for extended time, which is not possible using bare TiO<sub>2</sub> due to the significant poisoning of active sites.

**Keywords:** TiO<sub>2</sub>; photocatalysis; toluene; surface deactivation

## 1. Introduction

Emission of volatile organic compounds (VOCs) is regarded as a serious problem in environmental science and engineering. Indoors, VOCs can be emitted from materials such as paints and adhesives, causing sick-building syndrome [1,2]. In outdoor environments, VOCs emitted from vehicles and power stations are not only harmful to humans by themselves, but also create particulate matter by reacting with NO<sub>x</sub> and sunlight [3,4].

Various methods can be applied to remove VOCs. Porous adsorbents (activated carbons, metal-organic-frameworks, and meso- and micro-porous materials with diverse chemical compositions) with high surface areas can be used to capture VOCs [5–8]. As a representative example of commercially available adsorbents, activated carbons are relatively cost-effective. As a result, activated carbon filters are widely used for purifying air in the indoor and outdoor atmosphere. In addition, adsorbents are advantageous for VOC removal because no energy source is needed in the VOC-capturing process.

However, adsorbents must be replaced once the surface adsorption sites of the adsorbents are all occupied by adsorbed molecules. Used adsorbents can be regenerated by heating; however, this process can create secondary emission of VOCs [9].

Alternatively, VOCs can be removed by catalysis, using either thermal (dark) or photocatalysts [10–14]. Recently, photocatalytic degradation of VOCs has been drawing much attention. Titanium oxide ( $\text{TiO}_2$ ) is the most widely used photocatalyst due to its chemical stability and cost-effectiveness [15–17]. Since  $\text{TiO}_2$  has a band gap of  $\sim 3.2$  eV, ultraviolet (UV) light sources are required to initiate photocatalytic processes on  $\text{TiO}_2$  surfaces [15–17]. Recently, UV light-emitting diodes have become less expensive, which has increased the attention on indoor air purification by  $\text{TiO}_2$ -based photocatalysis. Once  $\text{TiO}_2$  is exposed to UV light with energy exceeding 3.2 eV, electron-hole pairs are created in  $\text{TiO}_2$ . The electron-hole pairs then interact with  $\text{O}_2$  and  $\text{H}_2\text{O}$  in the atmosphere, forming strong oxidizing agents such as  $\text{O}_2^-$  and  $\text{OH}^\cdot$  radicals, which can decompose organic molecules in the atmosphere [15,16].

In photocatalysis, the catalytic active sites on the surface can be easily covered by reaction intermediates, particularly during photocatalytic oxidation of relatively large and stable molecules such as benzene and toluene. Photocatalytic oxidation of those large molecules often involves the formation of various partially oxidized species that are recalcitrant to further oxidization into  $\text{CO}_2$  and  $\text{H}_2\text{O}$  due to their high stability. Therefore, deactivation of the photocatalytic surface is much more pronounced during the photocatalytic degradation of larger molecules than of smaller molecules [18]. In previous works, the reaction rate of photocatalytic decomposition of toluene was found to drastically decrease with reaction time, and poisoning of the  $\text{TiO}_2$  surface by partially oxidized species of toluene such as benzoic acid or benzaldehyde was found to be responsible for this deactivation phenomenon [18]. Many attempts have been made to alleviate such poisoning problems by modifying the surface structure of  $\text{TiO}_2$  [19–22].  $\text{TiO}_2$  nanotubes were found to facilitate the approach of oxygen molecules toward the surface active sites of  $\text{TiO}_2$  compared to thin films consisting of  $\text{TiO}_2$  nanoparticles with random shapes, thereby increasing the oxidation rate and reducing poisoning during the photocatalytic oxidation of toluene. Such methods, however, require significant development before they will be ready for commercial use [20].

In the present work, we modified the surface of commercially available  $\text{TiO}_2$  nanoparticles (P-25, Evonik) using a polydimethylsiloxane (PDMS) coating and subsequent annealing. We have recently shown that our methods of PDMS coating on nanoparticles can be easily scaled up [23–27]. We show that hydrophilically-modified  $\text{TiO}_2$  (hereafter referred to as h- $\text{TiO}_2$ ) is much more resistant to poisoning during photocatalytic decomposition of toluene compared to bare  $\text{TiO}_2$ . The mechanism of the poisoning-resistant behavior of h- $\text{TiO}_2$  is discussed in detail. We conclude that h- $\text{TiO}_2$  has high potential for application in photocatalytic air purification.

## 2. Results and Discussion

### 2.1. Characterizations of Samples

Figure 1 shows the XPS data for bare  $\text{TiO}_2$ , PDMS-coated  $\text{TiO}_2$  (coating temperature: 180 °C), and vacuum-annealed  $\text{TiO}_2$  (h- $\text{TiO}_2$ ). In the C 1s spectra shown in Figure 1a, PDMS deposition results in a negative chemical shift of the peak. Bare  $\text{TiO}_2$  should be free from any carbon in principle, yet some carbon impurities can always be found on samples that have been exposed to air. Carbon atoms observed on bare  $\text{TiO}_2$  can be attributed to those in amorphous carbon structures with  $\text{sp}^2$  or  $\text{sp}^3$  hybridizations [28–30]. The C 1s signal of PDMS-coated  $\text{TiO}_2$  can be attributed mostly to C atoms from the PDMS framework [28–30]. The carbon impurities originally present on  $\text{TiO}_2$  can be oxidized and removed during PDMS coating at 180 °C under air. After vacuum annealing of the PDMS-coated  $\text{TiO}_2$ , additional shoulders at higher binding energies appeared, which is indicative of the formation of C-OH and C=O [28–30]. Formation of such functional groups in the vacuum-annealed sample was verified by FT-IR measurements [28,31], which resulted in the improved hydrophilicity of h- $\text{TiO}_2$  compared to bare  $\text{TiO}_2$  particles. h- $\text{TiO}_2$  particles were mostly dispersed in water as they were dispersed into

a bi-layer heterogeneous mixture consisting of toluene and water, whereas bare  $\text{TiO}_2$  particles were dispersed both into toluene and water under the same conditions (Supporting Information 7).

In the O 1s core level spectra (Figure 1b), bare  $\text{TiO}_2$  showed features of the lattice oxygen of  $\text{TiO}_2$  at lower binding energies, as well as some hydroxyl groups on the surface at higher binding energies [29,30]. Upon PDMS coating, a peak centered at 531.5 eV became pronounced, originating from PDMS [29,30]. Upon subsequent annealing, peaks at higher binding energies corresponding to  $-\text{OH}$ ,  $\text{C}=\text{O}$  can be observed, together with a small peak at 533 eV, attributed to  $\text{SiO}_x$  due to the oxidation of Si atoms in PDMS [29,30]. In the Si 2p spectra (Figure 1c), the PDMS-coated surface showed features of Si(II), corresponding to that of PDMS [29,30]. Upon annealing, the Si 2p peak intensity became smaller, which indicates that much of the PDMS was desorbed from the surface of  $\text{TiO}_2$ . Some broad features, which can be attributed to  $\text{SiO}_x$ , were identified in the Si 2p spectrum of the vacuum-annealed sample. The Ti 2p spectra of all samples showed the doublet feature of Ti(IV) due to spin-orbit coupling, without any indication of lower oxidation numbers of Ti in any sample [29,30]. In the UV/VIS DRS spectra, h- $\text{TiO}_2$  showed absorption of visible light, which indicates the presence of Ti(III) and Ti atoms with even lower oxidation numbers (Supporting Information 2). The optical band gap of bare  $\text{TiO}_2$  and h- $\text{TiO}_2$  were determined using Kubelka-Munk method [32,33], and they are 3.2 and 3.1 eV, respectively (Supporting Information 2). However, this was not verified by the Ti 2p spectra in XPS. It seems that oxygen vacancies creating lower oxidation numbers in nearby Ti atoms can be found in deeper layers of  $\text{TiO}_2$  far from the surface. Please note that XPS is only surface sensitive, whereas UV/VIS monitors many layers deeper [34]. We believe that the lattice oxygen of  $\text{TiO}_2$  is used to partially oxidize the PDMS upon vacuum annealing, yet this results in subsurface or bulk oxygen vacancies rather than vacancies at the surface.

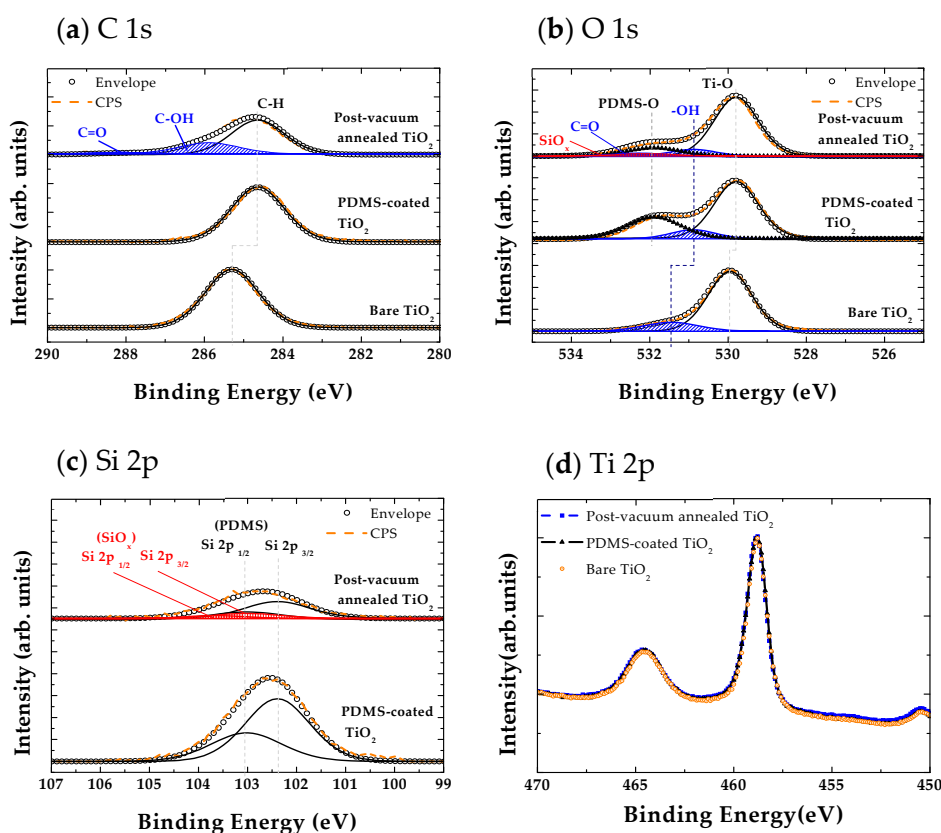


**Figure 1.** (a) C 1s and (b) O 1s XPS spectra of bare  $\text{TiO}_2$ , PDMS-coated  $\text{TiO}_2$ , and vacuum-annealed  $\text{TiO}_2$ . (c) Si 2p XPS spectra of PDMS-coated  $\text{TiO}_2$  and vacuum-annealed  $\text{TiO}_2$ . (Note that the area of every spectrum is normalized to the respective Ti 2p area.) (d) Ti 2p XPS spectra of bare  $\text{TiO}_2$ , PDMS-coated  $\text{TiO}_2$ , and vacuum-annealed  $\text{TiO}_2$ .

## 2.2. Photocatalytic Decomposition of Toluene under Dry Conditions

We conducted photocatalytic decomposition of toluene experiments under dry air with an initial toluene concentration of 66 ppm using a batch reactor. Bare  $\text{TiO}_2$  and h- $\text{TiO}_2$  were used as photocatalysts. For each sample, the reaction was repeated three times. After the first ~10 h reaction was completed, the reactor was evacuated and then refilled with dry air and 66 ppm of toluene, and the photocatalysis experiment was conducted again. This whole process was repeated again after the second photocatalysis experiment was finished. Results using these two different photocatalysts are summarized in Figure 2 and Supporting Information 3.

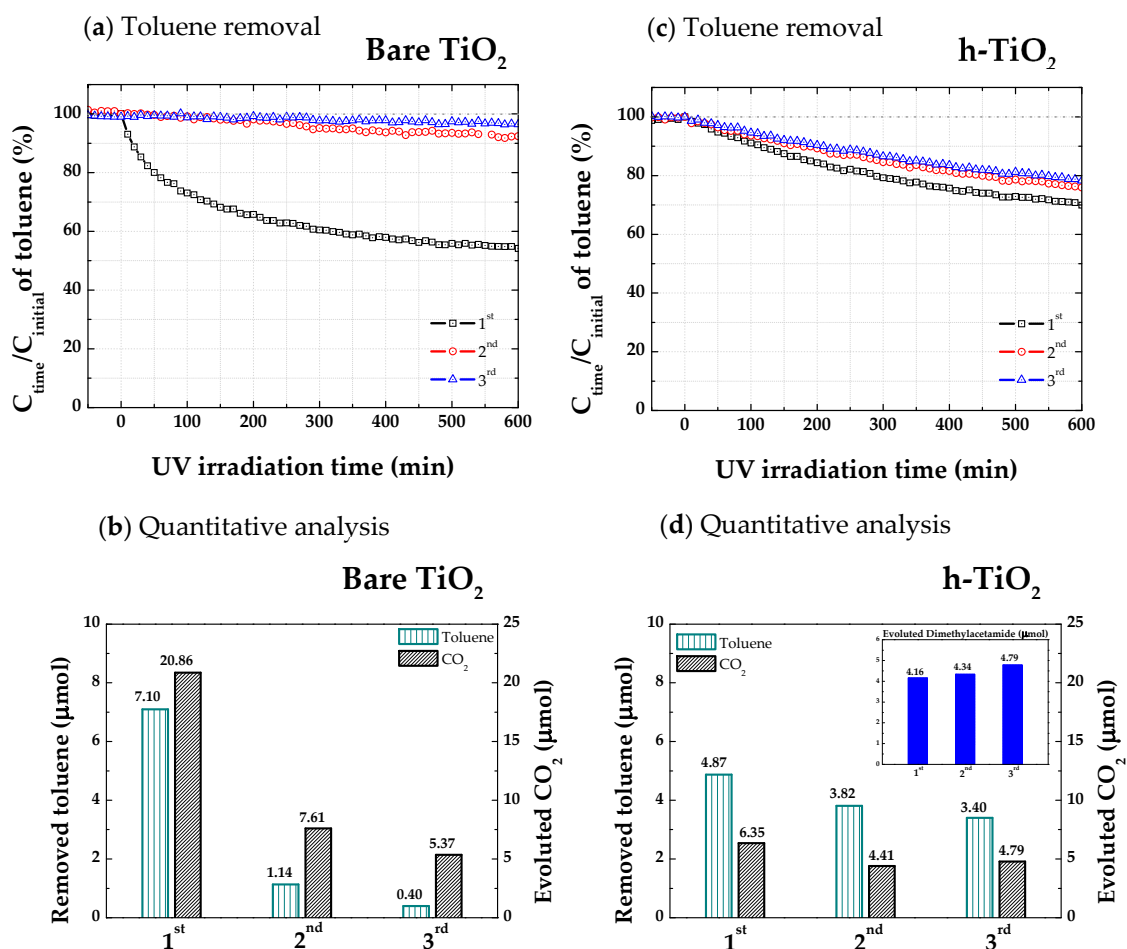


**Figure 2.** (a) Changes in toluene concentration under dry conditions over bare  $\text{TiO}_2$  as a function of UV irradiation time. Each reaction experiment was performed under dry conditions and an initial toluene concentration of 66 ppm. The photocatalytic decomposition experiment was repeated three times without changing the catalyst sample. (b) Comparison of total removed toluene and total evolved  $\text{CO}_2$  after 600 min of UV irradiation of each experiment in (a). Note that the y-scales are different for each species. (c) Changes in toluene concentration under dry conditions over h- $\text{TiO}_2$  as a function of UV irradiation time. (d) Comparison of total removed toluene, total evolved  $\text{CO}_2$ , and total evolved dimethylacetamide (inset) after 600 min of UV irradiation of each experiment in (c).

When bare  $\text{TiO}_2$  was used as the photocatalyst, the decomposition rate of toluene during the first reaction dramatically decreased over time; after 500 min of UV irradiation, almost no further removal of toluene could be observed. Please note that the slope (first order derivative value) of a specific time-period in a curve of Figure 2a corresponds to the temporary reaction rate. Carbon dioxide evolution could also be observed over time during the first reaction (Supporting Information 3), although the amount of produced  $\text{CO}_2$  was much less than expected assuming that toluene completely

oxidizes into  $\text{CO}_2$  and  $\text{H}_2\text{O}$ . Obviously, a large portion of the toluene molecules was not completely oxidized into  $\text{CO}_2$  and  $\text{H}_2\text{O}$ , but only partially oxidized (most likely into benzaldehyde and benzoic acid, as shown in previous studies). The catalyst surface was covered by these partially oxidized species, resulting in gradual reduction in the photocatalytic removal rate of toluene and  $\text{CO}_2$  evolution rate over time [18]. In the subsequent photocatalytic experiments, almost no removal of toluene could be detected. This suggests that, over the course of the first experiment, the bare  $\text{TiO}_2$  surface was already mostly deactivated by the partially oxidized species of toluene occupying the active sites of the  $\text{TiO}_2$  photocatalyst.

The amounts of removed toluene and evolved  $\text{CO}_2$  in the three successively performed photocatalysis experiments are summarized in Figure 2b. The initial concentration (ppm) of toluene was determined by the relative partial pressure of toluene to total pressure of gas mixture, whereas the number of toluene molecules ( $\mu\text{mol}$ ) was calculated based on the perfect gas law considering the total volume of the reactor (5.3 L). The number of  $\text{CO}_2$  molecules in the reactor was calculated based on a linear relationship between the number of carbon atoms existing in an injected gas and FID (Flame Ionization Detector) peak intensity of GC (Gas Chromatography). More details on the calculation process of each value can be found in Supporting Information 8. In the first photocatalytic decomposition experiment of toluene with bare  $\text{TiO}_2$ , the total amount of removed toluene was 7.10  $\mu\text{mol}$ , and the total amount of evolved  $\text{CO}_2$  was 20.86  $\mu\text{mol}$ . Considering that one completely mineralized toluene molecule generates 7 molecules of gaseous  $\text{CO}_2$ , it appears that less than half of the removed toluene molecules were totally oxidized. The rest of the toluene molecules can be assumed to be partially oxidized and covering the surface. It is worth noting that, even though almost no removal of toluene was observed in the second and third experiments, some evolution of  $\text{CO}_2$  was detected. It seems that some portion of the partially oxidized species of toluene remaining on the surface were slowly oxidized further, yielding  $\text{CO}_2$  and  $\text{H}_2\text{O}$ , yet rearrangement of the structure of the partially oxidized species did not seem to create free active sites available for adsorption and photocatalytic decomposition of additional toluene molecules from the gas phase in the second and third experiments.

In Figure 2c,d, the results of the photocatalytic decomposition of toluene using h- $\text{TiO}_2$  photocatalysts are demonstrated. Compared to the results of the first photocatalytic decomposition experiment of bare  $\text{TiO}_2$ , h- $\text{TiO}_2$  shows less photocatalytic activity toward toluene than bare  $\text{TiO}_2$  in terms of average photocatalytic decomposition rate, total amount of toluene removed, and total  $\text{CO}_2$  evolved (Supporting Information 3). However, the pronounced deactivation of the photocatalyst observed for bare  $\text{TiO}_2$  in the repeated experiments was not observed with h- $\text{TiO}_2$ . Therefore, when one compares the results of the second and third photocatalysis experiments for the two different samples, h- $\text{TiO}_2$  is suggested to be a superior photocatalyst to bare  $\text{TiO}_2$ .

Regarding the reaction products of photocatalytic decomposition of toluene using h- $\text{TiO}_2$ , there was a second reaction product in addition to  $\text{CO}_2$ , which was identified by GC. With aid of ex-situ GC/MS (Gas Chromatography/Mass Spectrometer) analysis, we identified the second product as dimethylacetamide (Supporting Information 4). It is suggested that the higher vapor pressure of dimethylacetamide than that of typical reaction intermediates of toluene (e.g., benzoic acid, benzyl aldehyde) allowed dimethylacetamide to be easily detached from the h- $\text{TiO}_2$  surface so that it remained active throughout the toluene photocatalytic decomposition. However, it is likely that not all produced dimethylacetamide was detected by the GC spectra or GC/MS analysis. Since dimethylacetamide has a much lower vapor pressure than toluene at room temperature, and because dimethylacetamide is quite polar, the molecules are likely to be easily adsorbed to the inner wall of the reactor. Therefore, we should scrutinize the quantitative analyses of the reaction yield of this toluene oxidation side reaction, as well as selectivity of h- $\text{TiO}_2$  for a specific reaction product. Figure 2d summarizes the total amounts of removed toluene, produced  $\text{CO}_2$ , and produced dimethylacetamide in the three successively performed experiments using h- $\text{TiO}_2$ . The deactivation of the photocatalyst in this case is much less pronounced than in the case of bare  $\text{TiO}_2$ . Particularly, the amount of produced dimethylacetamide is almost uniform between each experiment.

### 2.3. Photocatalytic Decomposition of Toluene under Humid Conditions

It was previously reported that deactivation of the TiO<sub>2</sub> surface during photocatalytic decomposition of toluene is less pronounced or not observed when the humidity of the atmosphere is relatively high and the initial toluene concentration is low [18]. It was proposed that, in high humidity, hydroxyl (OH) radical formation is facilitated by the interaction between water vapor in the atmosphere and the holes created by the optical excitation of TiO<sub>2</sub>. Hydroxyl radicals are known to act as oxidizing agents and are particularly effective in oxidizing various carbon-containing species chemisorbed on the TiO<sub>2</sub> surface into CO<sub>2</sub> and H<sub>2</sub>O [18,35].

As one can see from Figure 3a, which shows the total amounts of removed toluene and produced CO<sub>2</sub> in each of the two successively performed photocatalysis experiments using bare TiO<sub>2</sub>, the number of moles of CO<sub>2</sub> produced is ~7 fold greater than the respective value of toluene removed, and there is no indication of deactivation in the subsequent photocatalysis experiments. It is worth emphasizing that the initial concentration of toluene in the experiments of Figure 3 was 66 ppm, which was the same value as that used for the experiments shown in Figure 2. The only difference in experimental conditions between Figures 2 and 3 is the relative humidity of the atmosphere, which are 0% and ~34%, respectively. In contrast to the results of the experiments under dry conditions shown in Figure 2a and Supporting Information 3, in which the toluene removal and CO<sub>2</sub> evolution rates in the first reaction experiment gradually decreased over time, the toluene removal and CO<sub>2</sub> evolution rates were not significantly reduced with time under humid conditions (Supporting Information 5). Our observation that no significant deactivation of TiO<sub>2</sub> photocatalyst surface occurs during toluene decomposition under high humidity is in line with previously reported results [18].

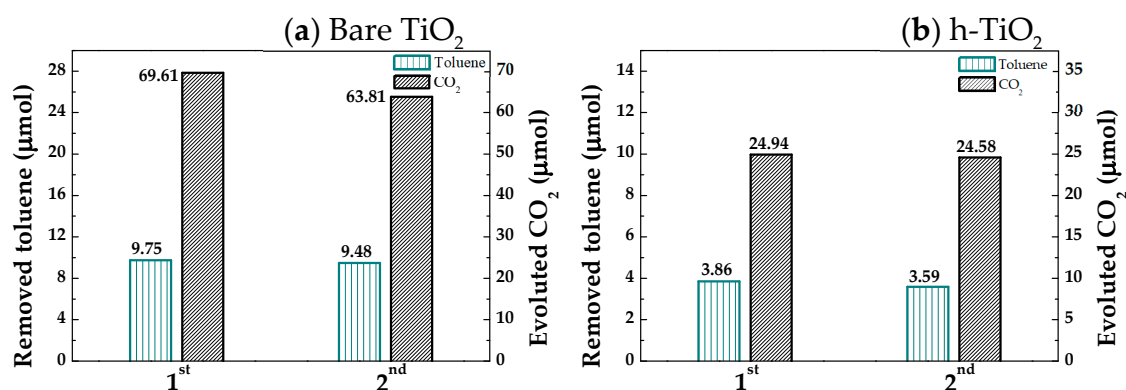


**Figure 3.** Photocatalytic decomposition experiments of toluene under high humidity. Each reaction experiment was conducted under high humidity (33.6% relative humidity) and an initial toluene concentration of 66 ppm. The photocatalytic decomposition experiment was repeated twice without changing the catalyst sample. (a) Comparison of total removed toluene and total evolved CO<sub>2</sub> after 600 min of UV irradiation of each experiment in the presence of bare TiO<sub>2</sub>. (b) Comparison of total removed toluene and total evolved CO<sub>2</sub> after 600 min of UV irradiation of each experiment in the presence of h-TiO<sub>2</sub>. Note that the y-scales are different for each species.

When h-TiO<sub>2</sub> was used for the toluene photocatalytic decomposition experiments under high humidity, there was again no indication of photocatalyst deactivation. Comparing the results of bare TiO<sub>2</sub> and h-TiO<sub>2</sub>, bare TiO<sub>2</sub> showed more toluene removal and CO<sub>2</sub> evolution activity under highly humid conditions than h-TiO<sub>2</sub>. Moreover, the formation of dimethylacetamide, which was observed during photocatalytic decomposition of toluene on h-TiO<sub>2</sub> under dry conditions as a side product (Figure 2 and Supporting Information 4), was suppressed by the increased humidity.

When the humidity of the atmosphere for the photocatalytic reaction was slightly reduced (from 34 to 25%) and the toluene initial concentration was greatly increased (from 66 to 442 ppm), for both bare TiO<sub>2</sub> and h-TiO<sub>2</sub>, the results were qualitatively analogous to those under dry conditions and lower toluene concentration (0 %RH and 66 ppm). As shown in Figure 4a and Supporting Information 6,

bare TiO<sub>2</sub> showed significant deactivation as the reaction progressed and across repeated experiments. Evolution of CO<sub>2</sub> was much less than the expected, according to the assumption of complete toluene mineralization. Obviously, the increased partial pressure of toluene dominated the adsorption sites on the surface of TiO<sub>2</sub>, reducing the probability of water chemisorption and OH radical formation.

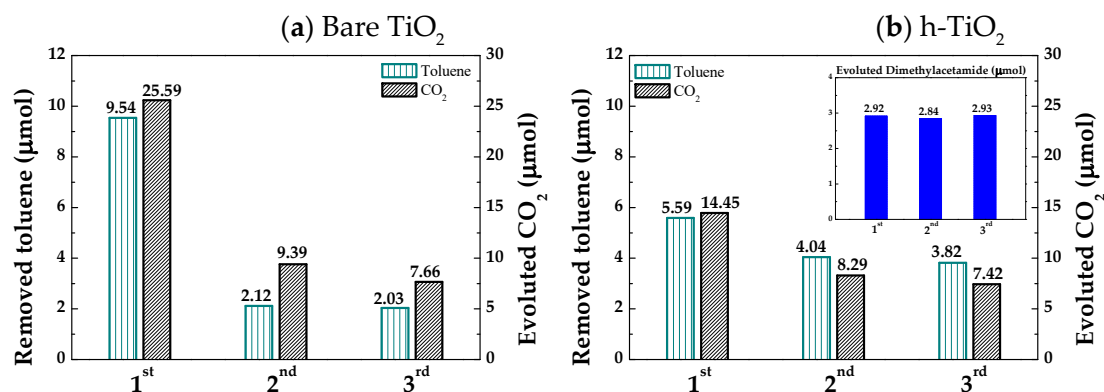


**Figure 4.** Photocatalytic decomposition experiments of toluene under high humidity with high initial toluene concentration. Each reaction experiment was conducted under high humidity (25.2% relative humidity) and an initial toluene concentration of 442 ppm. The photocatalytic decomposition experiment was repeated three times without changing the catalyst sample. (a) Comparison of total removed toluene and total evolved CO<sub>2</sub> after 600 min of UV irradiation of each experiment in the presence of bare TiO<sub>2</sub>. (b) Comparison of total removed toluene, total evolved CO<sub>2</sub>, and total evolved dimethylacetamide (inset) after 600 min of UV irradiation of each experiment in the presence of h-TiO<sub>2</sub>. Note that the y-scales are different for each species.

The results for h-TiO<sub>2</sub> given the same reaction conditions were also analogous to results under dry conditions (Figure 4b). A slight degree of deactivation was indicated between the first and second photocatalysis experiments, yet the second and third experiments showed almost identical catalytic activity for the decomposition of toluene and evolution of CO<sub>2</sub>. In addition, dimethylacetamide formation was observed, similar to the results of Figure 2d under dry conditions, which is quantitatively almost the same as the three successively performed photocatalysis experiments.

#### 2.4. Proposed Surface Structure of h-TiO<sub>2</sub>

Figure 5 illustrates a model of the surface structure of h-TiO<sub>2</sub>, which reconciles all the results of the photocatalysis experiments shown in Figures 2–4 and Supporting Information 3–6. We propose that the h-TiO<sub>2</sub> surface consists of two different domains. One domain has an identical atomic surface structure to that of bare TiO<sub>2</sub>, whereas the second domain consists of hydrophilic surface functional groups (such as hydroxyl, aldehyde, or carboxyl groups) bound to Si atoms originating from PDMS. It is worth mentioning that the formation of very thin films of PDMS (thickness of ~1 nm) on various substrates via the presented TVD (Thermal Vapor Deposition) method had been previously proved [26,28,36]. Besides, the re-vaporization of deposited PDMS thin films from its substrates by annealing at temperature above 400 °C under dry air condition was also evidenced by our previous results of TGA (Thermo-Gravimetric Analysis) analysis [37]. Therefore, it is likely that some of deposited PDMS films (thickness of ~1 nm) were re-vaporized from TiO<sub>2</sub> particles in the post-annealing process of the present study (at 800 °C, under vacuum condition), forming the bare TiO<sub>2</sub> domains. We would like to mention that the ratio XPS peak intensity of Si 2p/Ti 2p decreased upon the post-annealing process, implying the re-opening of bare TiO<sub>2</sub> domain by the re-vaporization of some of PDMS films (Figure 1c).

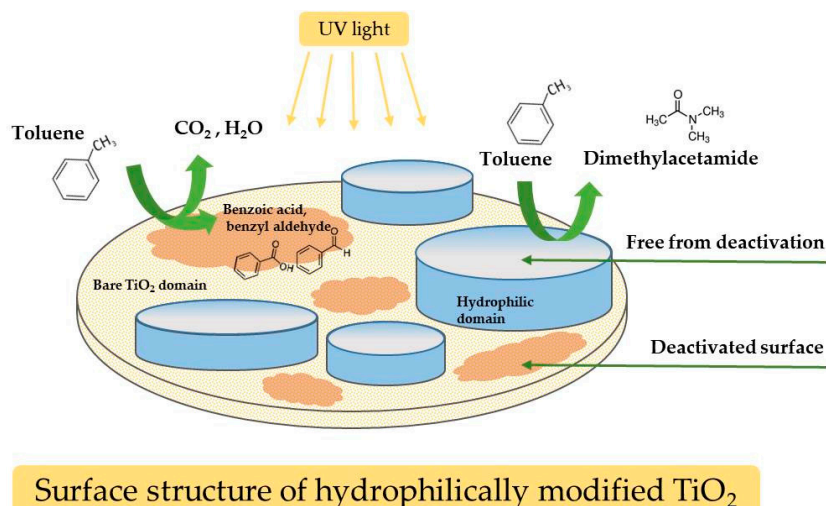


**Figure 5.** Schematic description of photocatalytic decomposition of toluene over the h-TiO<sub>2</sub> surface.

Under dry conditions with lower toluene concentrations (0 %RH and 66 ppm of toluene) and humid condition with very high toluene concentrations (25 %RH and 442 ppm of toluene), the h-TiO<sub>2</sub> surface showed some deactivation of the surface domain with the same structure as bare TiO<sub>2</sub>. Under these conditions, h-TiO<sub>2</sub> also formed dimethylacetamide through the catalytic reactions taking place on the hydrophilic domain. Since the hydrophilic domain preferentially adsorbs water molecules over toluene compared to bare TiO<sub>2</sub>, the catalytic reactions resulting in the formation of dimethylacetamide on the hydrophilic domain could be fully suppressed under high humidity and low toluene concentration conditions. In other words, toluene and water molecules competitively adsorb onto the hydrophilic domain surfaces, and the photocatalytic decomposition of toluene toward the formation of dimethylacetamide can only be found when toluene can chemisorb onto that surface.

The lower rate of toluene removal on h-TiO<sub>2</sub> surface than on bare TiO<sub>2</sub> was observed at the initial stage of photocatalytic reaction, especially when dimethylacetamide formation was found (Figures 2 and 4), and this can be also understood based on the proposed surface structure of h-TiO<sub>2</sub> sample. There is an additional reaction path of toluene removal on h-TiO<sub>2</sub> surface compared to the case of bare TiO<sub>2</sub>; toluene conversion to CO<sub>2</sub> on the surface of bare TiO<sub>2</sub> domain and the conversion of toluene to dimethylacetamide on the hydrophilic domain. The initial reaction rate of the dimethylacetamide formation on hydrophilic domain was lower than the CO<sub>2</sub> formation on bare TiO<sub>2</sub> domain, resulting in the lower overall rate of toluene removal on the surface of h-TiO<sub>2</sub> compared to the case of bare TiO<sub>2</sub> at initial stage of the photocatalytic reaction. It is worth noting that only slight deactivation of photocatalytic activity of h-TiO<sub>2</sub> was observed in the repeatedly performed experiments whereas the photocatalytic activity of bare TiO<sub>2</sub> was significantly reduced when the experiments were repeated under the same conditions (Figures 2 and 4). On h-TiO<sub>2</sub>, both domains (bare and hydrophilic domains) exist, yet the bare TiO<sub>2</sub> domain is rapidly deactivated and therefore the main reaction path on h-TiO<sub>2</sub> surface in an extended time period is dominated by hydrophilic domains, where toluene is converted into dimethylacetamide. Bare TiO<sub>2</sub> domain is only active at the very early stage of the photocatalysis experiment.

The molecular-level mechanism for the formation of dimethylacetamide from toluene warrants further study and possibly theoretical works in the future. In any case, formation of dimethylacetamide indicates the activation of N<sub>2</sub> molecules on the hydrophilic domains of h-TiO<sub>2</sub>. In this context, it is worth mentioning that ammonia formation from N<sub>2</sub> and H<sub>2</sub> has been observed using some photocatalysts in previous studies [38].

Unfortunately, dimethylacetamide is also regarded to be harmful to animals and human beings to some extent [39]. However, dimethylacetamide shows lower vapor pressure than toluene and quite high solubility in liquid water [40]. Therefore, removal of dimethylacetamide using an additional apparatus in tandem with the photocatalytic air purifier is feasible. More importantly, bare TiO<sub>2</sub>

suffers from deactivation during photocatalytic decomposition of aromatic compounds such as toluene and shows reduced activity for all other VOCs (such as acetaldehyde and formaldehyde) with time. In contrast, h-TiO<sub>2</sub> can maintain its photocatalytic activity for a long time even after exposure to toluene vapor under UV irradiation.

### 3. Materials and Methods

#### 3.1. Sample Preparation

The first step of hydrophilic surface modification is thermal deposition of PDMS on TiO<sub>2</sub> nanoparticles. The schematic description of the process is shown in Figure 6a. A stainless-steel chamber with a volume of 2.2 L was used as a reactor. A fluid amount of 30 g PDMS (1000 cs, Xiameter, Midland, MI, USA) was loaded into a container made of aluminum foil with a lateral size of 5 cm × 7 cm, which was then placed on the bottom of the chamber. 10 g of commercial TiO<sub>2</sub> nanoparticles (P-25, Evonik, Essen, Germany) was loaded into a container made of stainless-steel mesh with a lateral size of 10.5 cm × 10 cm, and the container was placed 5 cm above the bottom of the chamber. The top part of the chamber was then covered with a stainless-steel lid. Polyimide (PI) tape was used to seal the gap between the chamber and the lid. The outside of the chamber was wrapped with a heating band, and the temperature of the chamber was monitored by a K-type thermocouple attached to the upper side of the chamber and was controlled using a thermo-regulator (SU-105K, Samwon Eng, Seoul, Korea).

The PDMS was deposited onto the TiO<sub>2</sub> nanoparticles at a chamber temperature of 180 °C, based on our previous works. The TiO<sub>2</sub> particles modified by PDMS coating at 180 °C and subsequent vacuum annealing showed the highest photocatalytic activity toward methylene blue and phenol molecules [29]. The temperature of the chamber was increased from room temperature to 180 °C and then kept at 180 °C for 12 h. After deposition, the chamber was cooled to room temperature, and the PDMS-coated sample was collected.

The next step of hydrophilic surface modification is vacuum annealing of the PDMS-coated TiO<sub>2</sub> powder, shown schematically in Figure 6b. PDMS-coated TiO<sub>2</sub> powder was loaded in the middle of a quartz tube and was fixed by placing quartz wool on either side of the powder. The quartz tube was evacuated with a rotary pump, and the pressure of the tube was maintained at 10<sup>-3</sup> torr during the process. The temperature of the tube was increased from room temperature to 800 °C within 2 h and maintained at 800 °C for another 2 h. After this process, the temperature was decreased to room temperature, and the vacuum-annealed TiO<sub>2</sub> sample was collected.

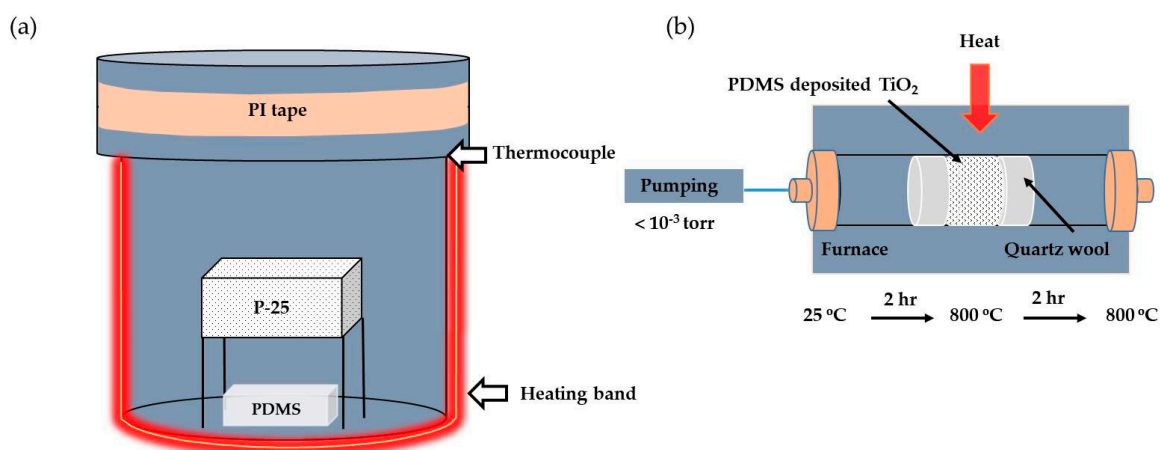


**Figure 6.** Schematic diagram of the experimental set-up for two-step hydrophilic surface modification: (a) deposition of PDMS on TiO<sub>2</sub> nanopowder at 180 °C, followed by (b) annealing of PDMS-coated TiO<sub>2</sub> at 800 °C under vacuum conditions.

### 3.2. Characterization

X-ray photoelectron spectroscopy (XPS) was used to analyze the surface of bare TiO<sub>2</sub>, PDMS-coated TiO<sub>2</sub>, and vacuum-annealed TiO<sub>2</sub> (h-TiO<sub>2</sub>). The XPS spectra were acquired with Mg-K $\alpha$  (1253.6 eV, X-ray source) and a hemispherical analyzer (PHOIBOS-Has 2500, SPECS, Berlin, Germany). The measurements were conducted in an ultra-high vacuum chamber with a base pressure of  $3.0 \times 10^{-10}$  torr at room temperature. Optical properties of bare TiO<sub>2</sub> and vacuum-annealed TiO<sub>2</sub> were analyzed on UV-Vis reflectance spectra in the wavelength range of 200–800 nm using a UV-Vis diffuse reflectance spectrometer (UV-Vis DRS, UV-3600, SHIMADZU, Kyoto, Japan). Reaction products were identified by ex-situ thermal desorption-gas chromatography mass spectrometry (TD-GC/MS). The gas mixture inside the reactor was collected in a tedlar bag and was adsorbed to a single-bed tube (Tenax<sup>®</sup> TA, Supelco, Bellefonte, PA, USA) by drawing 50 sccm from the bag into the tube for 20 min using a mass flow controller. The single-bed tube was then heated to 280 °C in a thermal desorption system (TDSA2, GERSTEL, Linthicum, MD, USA) to desorb the gas mixture, and the desorbed gas mixture was injected into a gas chromatograph (5975 series, Agilent, Santa Clara, CA, USA) equipped with a capillary column (DB-1MS, 60.0 m  $\times$  250.00  $\mu$ m, Agilent Technologies) and an inert quadrupole-type mass selective detector.

### 3.3. Photocatalytic Reactions

Photocatalytic decomposition of toluene was carried out over the surface of bare TiO<sub>2</sub> or h-TiO<sub>2</sub> film on an SUS (stainless steel) plate. The method for film preparation is explained in detail elsewhere [35]. A high vacuum chamber (base pressure of  $\sim 10^{-5}$  torr) connected to a gas injection line and a gas chromatograph (GC, HP 6890 series, Hewlett Packard, Palo Alto, CA, USA) was used as a batch-type reactor. The top part of the chamber was closed with a viewport made of quartz. The gas injection line was connected to three gas bottles of dry air, toluene, and water vapor through leak valves. The GC was equipped with a 6-port valve (loop volume of 1 mL), and the valve was connected to the chamber by a polytetrafluoroethylene (PTFE) tube. A diaphragm pump (DA70EEAC, flow rate of 7 L/min, YLKTECH, Wuhan, China) was connected to the PTFE tube for fluent circulation of the gas mixture in the reactor. The total volume of the reactor (including the PTFE tube) was 5.3 L. The high vacuum chamber was also connected to another chamber equipped with a quadrupole mass spectrometer (QMS, HAL 201, HIDEN, Warrington, UK), in order to verify the purities of the three gases. See Supporting Information 1 for a schematic description of the experimental set-up.

Bare TiO<sub>2</sub> or h-TiO<sub>2</sub> film on an SUS plate was loaded into the high vacuum chamber. Three different gases were introduced into the reactor, and the pressure of the reactor was recorded through a Pirani vacuum gauge (SUPER BEE, InstruTech, Longmont, CO, USA). First, toluene gas (50, 450 mtorr) was injected into the reactor, followed by water vapor (8 and 6 torr of water vapor correspond to 33.6% and 25.2% relative humidity at 25 °C, respectively). Lastly, the reactor was filled with dry air until the total pressure reached 760 torr. After the gas injection was complete, the gas injection line was closed and separated from the reactor with an angle valve. Next, the diaphragm pump was turned on to circulate the gas mixture in the reactor. The gas mixture was pre-circulated for 30 min to ensure homogeneity throughout the entire volume of the reactor. After the pre-circulation, 1 mL of gas mixture was injected into the GC every 10 min to measure the change in concentration of each gaseous species over the reaction time. The GC was equipped with a capillary column (30.0 m  $\times$  320  $\mu$ m, DB-5, Agilent Technologies), a methanizer, and a flame ionization detector. After 100 min of pre-adsorption in the dark, UV light (365 nm wavelength) was irradiated onto the surface of the bare TiO<sub>2</sub> or h-TiO<sub>2</sub> through the quartz viewport using UV LED (500 mA of forward current, CUN6AF1B, Seoulviosys, Ansan, Korea). Distance between the light source and the sample was 9 cm.

## 4. Conclusions

We modified the surface of TiO<sub>2</sub> nanoparticles by thermal deposition of polydimethylsiloxane followed by annealing under vacuum conditions. This process yielded hydrophilic functional groups

on the surface of TiO<sub>2</sub>. Then, we compared the UV light-driven photocatalytic activities of bare TiO<sub>2</sub> and hydrophilically-modified TiO<sub>2</sub> (h-TiO<sub>2</sub>) for the toluene decomposition reaction under various conditions. Bare TiO<sub>2</sub> showed significant surface deactivation under dry conditions with low initial toluene concentrations (66 ppm), which is ascribed to the accumulation of partially oxidized toluene species (benzylaldehyde, benzoic acid) on the catalyst surface. In addition, under humid (25.2%) conditions with very high initial toluene concentration (442 ppm), the surface deactivation was also obvious. In contrast, under high humidity (33.6%) with low initial toluene concentration (66 ppm), wherein the number of water molecules is much greater than the number of gaseous toluene molecules, the surface deactivation was not significant. When h-TiO<sub>2</sub> was used as photocatalyst, such surface deactivation was not observed under the conditions where the deactivation of bare TiO<sub>2</sub> was significant. Under those conditions, toluene was converted to dimethylacetamide, which has a higher vapor pressure than that of other partially oxidized species and so did not stick to the surface or show surface deactivation. We propose that the h-TiO<sub>2</sub> surface consists of two different domains: a bare TiO<sub>2</sub> surface domain and a hydrophilic surface domain decorated with hydrophilic functional groups. In the bare TiO<sub>2</sub> surface domain, the surface deactivation is pronounced when the proportion of gaseous toluene molecules dominates the proportion of water molecules, whereas the hydrophilic surface domain is resistant to any surface deactivation. We believe that our h-TiO<sub>2</sub> has a high potential for application in air purification for extended reaction times without significant surface deactivation during reaction.

**Supplementary Materials:** The materials are available online at <http://www.mdpi.com/2073-4344/8/11/500/s1>.

**Author Contributions:** Conceptualization, B.J.C. and Y.D.K.; methodology, T.G.W.; software, B.J.C.; validation, B.J.C. and T.G.W.; formal analysis, B.J.C., and T.G.W.; investigation, B.J.C., and S.W.H.; resources, S.W.H., S.S., H.K.C., and J.Y.K.; data curation, B.J.C.; writing—original draft preparation, B.J.C.; writing—review and editing, H.O.S., Y.D.K.; visualization, B.J.C.; supervision, H.O.S., and Y.D.K.; project administration, H.O.S., and Y.D.K.; funding acquisition, H.O.S., and Y.D.K.

**Funding:** This work was supported by Basic Science Research Program through the National Research Foundation of Korea (NRF) funded by the Ministry of Education (2018R1D1A1B07040916) and also supported by the Basic Science Research Program through the National Research Foundation of Korea (NRF) funded by the Ministry of Education (2017R1D1A1B03034381). The authors would like to acknowledge the financial support from the Global Frontier Center for Hybrid Interface Materials (GFHIM) (Grant No. NRF-2013M3A6B1078879). B.J.C. was supported by Hyundai Motor Chung Mong-Koo Foundation.

**Conflicts of Interest:** The authors declare no conflict of interest.

## References

1. Gupta, S.; Khare, M.; Goyal, R. Sick building syndrome—A case study in a multistory centrally air-conditioned building in the Delhi city. *Build. Environ.* **2007**, *42*, 2797–2809. [[CrossRef](#)]
2. Jones, A.P. Indoor air quality and health. *Atmos. Environ.* **1999**, *33*, 4535–4564. [[CrossRef](#)]
3. Atkinson, R. Atmospheric chemistry of VOCs and NO<sub>x</sub>. *Atmos. Environ.* **2000**, *34*, 2063–2101. [[CrossRef](#)]
4. Odum, J.R.; Jungkamp, T.P.W.; Griffin, R.J.; Flagan, R.C.; Seinfeld, J.H. The atmospheric aerosol-forming potential of whole gasoline vapor. *Science* **1997**, *276*, 96–99. [[CrossRef](#)] [[PubMed](#)]
5. Zhao, X.S.; Ma, Q.; Lu, G.Q.M. VOC removal: Comparison of MCM-41 with hydrophobic zeolites and activated carbon. *Energy Fuels* **1998**, *12*, 1051–1054. [[CrossRef](#)]
6. Yang, K.; Sun, Q.; Xue, F.; Lin, D.H. Adsorption of volatile organic compounds by metal-organic frameworks MIL-101: Influence of molecular size and shape. *J. Hazard. Mater.* **2011**, *195*, 124–131. [[CrossRef](#)] [[PubMed](#)]
7. Das, D.; Gaur, V.; Verma, N. Removal of volatile organic compound by activated carbon fiber. *Carbon* **2004**, *42*, 2949–2962. [[CrossRef](#)]
8. Gil, R.R.; Ruiz, B.; Lozano, M.S.; Martin, M.J.; Fuente, E. VOCs removal by adsorption onto activated carbons from biocollagenic wastes of vegetable tanning. *Chem. Eng. J.* **2014**, *245*, 80–88. [[CrossRef](#)]
9. Dettmer, K.; Engewald, W. Adsorbent materials commonly used in air analysis for adsorptive enrichment and thermal desorption of volatile organic compounds. *Anal. Bioanal. Chem.* **2002**, *373*, 490–500. [[CrossRef](#)] [[PubMed](#)]

10. Carabineiro, S.A.C.; Chen, X.; Martynyuk, O.; Bogdanchikova, N.; Avalos-Borja, M.; Pestryakov, A.; Tavares, B.; Orfao, J.J.M.; Pereira, M.F.R.; Figueiredo, J.L. Gold supported on metal oxides for volatile organic compounds total oxidation. *Catal. Today* **2015**, *244*, 103–114. [[CrossRef](#)]
11. Jeong, M.G.; Park, E.J.; Jeong, B.; Kim, D.H.; Kim, Y.D. Toluene combustion over NiO nanoparticles on mesoporous SiO<sub>2</sub> prepared by atomic layer deposition. *Chem. Eng. J.* **2014**, *237*, 62–69. [[CrossRef](#)]
12. Mamaghani, A.H.; Haghighat, F.; Lee, C.S. Photocatalytic oxidation technology for indoor environment air purification: The state-of-the-art. *Appl. Catal. B Environ.* **2017**, *203*, 247–269. [[CrossRef](#)]
13. Delimaris, D.; Ioannides, T. VOC oxidation over MnO<sub>x</sub>-CeO<sub>2</sub> catalysts prepared by a combustion method. *Appl. Catal. B Environ.* **2008**, *84*, 303–312. [[CrossRef](#)]
14. Liotta, L.F. Catalytic oxidation of volatile organic compounds on supported noble metals. *Appl. Catal. B Environ.* **2010**, *100*, 403–412. [[CrossRef](#)]
15. Fujishima, A.; Zhang, X.T.; Tryk, D.A. TiO<sub>2</sub> photocatalysis and related surface phenomena. *Surf. Sci. Rep.* **2008**, *63*, 515–582. [[CrossRef](#)]
16. Gaya, U.I.; Abdullah, A.H. Heterogeneous photocatalytic degradation of organic contaminants over titanium dioxide: A review of fundamentals, progress and problems. *J. Photochem. Photobiol. C* **2008**, *9*, 1–12. [[CrossRef](#)]
17. Tong, H.; Ouyang, S.X.; Bi, Y.P.; Umezawa, N.; Oshikiri, M.; Ye, J.H. Nano-photocatalytic materials: Possibilities and challenges. *Adv. Mater.* **2012**, *24*, 229–251. [[CrossRef](#)] [[PubMed](#)]
18. Jeong, M.G.; Park, E.J.; Seo, H.O.; Kim, K.D.; Kim, Y.D.; Lim, D.C. Humidity effect on photocatalytic activity of TiO<sub>2</sub> and regeneration of deactivated photocatalysts. *Appl. Surf. Sci.* **2013**, *271*, 164–170. [[CrossRef](#)]
19. Nakajima, A.; Obata, H.; Kameshima, Y.; Okada, K. Photocatalytic destruction of gaseous toluene by sulfated TiO<sub>2</sub> powder. *Catal. Commun.* **2005**, *6*, 716–720. [[CrossRef](#)]
20. Weon, S.; Choi, W. TiO<sub>2</sub> nanotubes with open channels as deactivation-resistant photocatalyst for the degradation of volatile organic compounds. *Environ. Sci. Technol.* **2016**, *50*, 2556–2563. [[CrossRef](#)] [[PubMed](#)]
21. Weon, S.; Kim, J.; Choi, W. Dual-components modified TiO<sub>2</sub> with Pt and fluoride as deactivation-resistant photocatalyst for the degradation of volatile organic compound. *Appl. Catal. B Environ.* **2018**, *220*, 1–8. [[CrossRef](#)]
22. Franch, M.I.; Peral, J.; Domenech, X.; Ayllon, J.A. Aluminium(III) adsorption: A soft and simple method to prevent TiO<sub>2</sub> deactivation during salicylic acid photodegradation. *Chem. Commun.* **2005**, *2015*, 1851–1853. [[CrossRef](#)] [[PubMed](#)]
23. Han, S.W.; Kim, K.D.; Seo, H.O.; Kim, I.H.; Jeon, C.S.; An, J.E.; Kim, J.H.; Uhm, S.; Kim, Y.D. Oil-water separation using superhydrophobic PET membranes fabricated via simple dip-coating of PDMS-SiO<sub>2</sub> nanoparticles. *Macromol. Mater. Eng.* **2017**, *302*, 1700218. [[CrossRef](#)]
24. Lee, J.H.; Park, E.J.; Kim, D.H.; Jeong, M.G.; Kim, Y.D. Superhydrophobic surfaces with photocatalytic activity under UV and visible light irradiation. *Catal. Today* **2016**, *260*, 32–38. [[CrossRef](#)]
25. Park, E.J.; Cho, Y.K.; Kim, D.H.; Jeong, M.G.; Kim, Y.H.; Kim, Y.D. Hydrophobic polydimethylsiloxane (PDMS) coating of mesoporous silica and its use as a preconcentrating agent of gas analytes. *Langmuir* **2014**, *30*, 10256–10262. [[CrossRef](#)] [[PubMed](#)]
26. Park, E.J.; Kim, K.D.; Yoon, H.S.; Jeong, M.G.; Kim, D.H.; Lim, D.C.; Kim, Y.H.; Kim, Y.D. Fabrication of conductive, transparent and superhydrophobic thin films consisting of multi-walled carbon nanotubes. *RSC Adv.* **2014**, *4*, 30368–30374. [[CrossRef](#)]
27. Park, E.J.; Yoon, H.S.; Kim, D.H.; Kim, Y.H.; Kim, Y.D. Preparation of self-cleaning surfaces with a dual functionality of superhydrophobicity and photocatalytic activity. *Appl. Surf. Sci.* **2014**, *319*, 367–371. [[CrossRef](#)]
28. Jeong, M.G.; Seo, H.O.; Kim, K.D.; Kim, Y.D.; Lim, D.C. Enhanced photocatalytic activity of TiO<sub>2</sub> by polydimethylsiloxane deposition and subsequent thermal treatment at 800 °C. *Thin Solid Films* **2012**, *520*, 4929–4933. [[CrossRef](#)]
29. Cha, B.J.; Woo, T.G.; Park, E.J.; Kim, I.H.; An, J.E.; Seo, H.O.; Kim, Y.D. Photo-catalytic activity of hydrophilic-modified TiO<sub>2</sub> for the decomposition of methylene blue and phenol. *Curr. Appl. Phys.* **2017**, *17*, 1557–1563. [[CrossRef](#)]
30. Moulder, J.F.; Stickle, W.F.; Sobol, P.E.; Bomben, K.D. *Handbook of X-ray Photoelectron Spectroscopy*; Physical Electronics Inc.: Chanhassen, MN, USA, 1995.
31. Park, E.J.; Jeong, B.; Jeong, M.G.; Kim, Y.D. Synergetic effects of hydrophilic surface modification and N-doping for visible light response on photocatalytic activity of TiO<sub>2</sub>. *Curr. Appl. Phys.* **2014**, *14*, 300–305. [[CrossRef](#)]

32. D'Amato, C.A.; Giovannetti, R.; Zannotti, M.; Rommozzi, E.; Ferraro, S.; Seghetti, C.; Minicucci, M.; Gunnella, R.; Di Cicco, A. Enhancement of visible-light photoactivity by polypropylene coated plasmonic Au/TiO<sub>2</sub> for dye degradation in water solution. *Appl. Surf. Sci.* **2018**, *441*, 575–587. [[CrossRef](#)]
33. D'Amato, C.A.; Giovannetti, R.; Zannotti, M.; Rommozzi, E.; Minicucci, M.; Gunnella, R.; Di Cicco, A. Band Gap Implications on Nano-TiO<sub>2</sub> Surface Modification with Ascorbic Acid for Visible Light-Active Polypropylene Coated Photocatalyst. *Nanomater. Basel* **2018**, *8*, 599. [[CrossRef](#)] [[PubMed](#)]
34. Woo, T.G.; Seo, H.O.; Kim, I.H.; Han, S.W.; Cha, B.J.; Kim, Y.D. Unveiling the complexity of the degradation mechanism of semiconducting organic polymers: Visible-light-induced oxidation of P3HT films on ZnO/ITO under atmospheric conditions. *J. Phys. Chem. C* **2017**, *121*, 18692–18701. [[CrossRef](#)]
35. Seo, H.O.; Park, E.J.; Kim, I.H.; Han, S.W.; Cha, B.J.; Woo, T.G.; Kim, Y.D. Influence of humidity on the photo-catalytic degradation of acetaldehyde over TiO<sub>2</sub> surface under UV light irradiation. *Catal. Today* **2017**, *295*, 102–109. [[CrossRef](#)]
36. Jeong, M.G.; Seo, H.O.; Kim, K.D.; Kim, D.H.; Kim, Y.D.; Lim, D.C. Quenching of photocatalytic activity and enhancement of photostability of ZnO particles by polydimethylsiloxane coating. *J. Mater. Sci.* **2012**, *47*, 5190–5196. [[CrossRef](#)]
37. Han, S.W.; Kim, I.H.; Kim, J.H.; Seo, H.O.; Kim, Y.D. Polydimethylsiloxane thin-film coating on silica nanoparticles and its influence on the properties of SiO<sub>2</sub>-polyethylene composite materials. *Polymer* **2018**, *138*, 24–32. [[CrossRef](#)]
38. Hirakawa, H.; Hashimoto, M.; Shiraishi, Y.; Hirai, T. Photocatalytic conversion of nitrogen to ammonia with water on surface oxygen vacancies of titanium dioxide. *J. Am. Chem. Soc.* **2017**, *139*, 10929–10936. [[CrossRef](#)] [[PubMed](#)]
39. Agency, E.C. *Opinion on N,N-Dimethylacetamide (DMAC)*; ECHA: Helsinki, Finland, 2014.
40. Lide, D.R.; Kehiaian, H.V. *CRC Handbook of Thermophysical and Thermochemical Data*; CRC Press: Boca Raton, FL, USA, 1994; p. 518.



© 2018 by the authors. Licensee MDPI, Basel, Switzerland. This article is an open access article distributed under the terms and conditions of the Creative Commons Attribution (CC BY) license (<http://creativecommons.org/licenses/by/4.0/>).